

Autocorrelations of stellar light and mass in the low-redshift Universe

Cheng Li^{1,2*} and Simon D. M. White¹

¹Max-Planck-Institute for Astrophysics, Karl-Schwarzschild-Str. 1, D-85741 Garching, Germany

²MPA/SHAO Joint Center for Astrophysical Cosmology at Shanghai Astronomical Observatory, Nandan Road 80, Shanghai 200030, China

Accepted Received; in original form

ABSTRACT

The final data release of the Sloan Digital Sky Survey (SDSS) provides reliable photometry and spectroscopy for about half a million galaxies with median redshift 0.09. Here we use these data to estimate projected autocorrelation functions $w_p(r_p)$ for the light of galaxies in the five SDSS photometric bands. Comparison with the analogous stellar mass autocorrelation, estimated in a previous paper, shows that stellar luminosity is less strongly clustered than stellar mass in all bands and on all scales. Over the full nonlinear range $10h^{-1}\text{kpc} < r_p < 10h^{-1}\text{Mpc}$ our autocorrelation estimates are extremely well represented by power laws. The parameters of the corresponding spatial functions $\xi(r) = (r/r_0)^\gamma$ vary systematically from $r_0 = 4.5h^{-1}\text{Mpc}$ and $\gamma = -1.74$ for the bluest band (the u band) to $r_0 = 5.8h^{-1}\text{Mpc}$ and $\gamma = -1.83$ for the reddest one (the z band). These may be compared with $r_0 = 6.1h^{-1}\text{Mpc}$ and $\gamma = -1.84$ for the stellar mass. Ratios of $w_p(r_p)$ between two given wavebands are proportional to the mean colour of correlated stars at projected distance r_p from a randomly chosen star. The ratio of the stellar mass and luminosity autocorrelations measures an analogous mean stellar mass-to-light ratio (M_*/L). All colours get redder and all mass-to-light ratios get larger with decreasing r_p , with the amplitude of the effects decreasing strongly to redder passbands. Even for the u -band the effects are quite modest, with maximum shifts of about 0.1 in $u - g$ and about 25% in M_*/L_u . These trends provide a precise characterisation of the well-known dependence of stellar populations on environment.

Key words: galaxies: clusters: general – galaxies: distances and redshifts – cosmology: theory – dark matter – large-scale structure of Universe.

1 INTRODUCTION

Over the past three decades, redshift surveys of nearby galaxies have established that galaxies of different types are distributed in space in different ways (e.g. Davis & Geller 1976; Dressler 1980). Among the various galaxy properties that have been considered, colour is found to be among the most dependent on local environment density (Kauffmann et al. 2004; Blanton et al. 2005), with luminosity also a significantly environment-dependent property (Blanton et al. 2005). Two-point autocorrelation functions, the traditional quantitative characterisation of clustering, thus depend both on luminosity (Davis et al. 1988; Hamilton 1988; White et al. 1988; Boerner et al. 1989; Einasto 1991; Park et al. 1994; Loveday et al. 1995; Benoist et al. 1996; Guzzo et al. 1997; Beisbart & Kerscher 2000; Norberg et al. 2001; Zehavi et al. 2002, 2005; Li et al. 2006; Skibba et al. 2006; Wang et al. 2007; Swanson et al.

2008) and on colour (Willmer et al. 1998; Brown et al. 2000; Zehavi et al. 2002, 2005; Li et al. 2006; Wang et al. 2007; Swanson et al. 2008; Skibba & Sheth 2009). Measurements of correlation functions for different classes of galaxies and with different weighting schemes provide powerful quantitative constraints on models of galaxy formation and evolution.

The Sloan Digital Sky Survey (SDSS; York et al. 2000) is the most ambitious optical imaging and spectroscopic survey to date. In Li & White (2009, hereafter Paper I) we studied the distribution of stellar mass in the local Universe using a complete and uniform sample of about half a million galaxies selected from the final data release (DR7; Abazajian et al. 2009) of the SDSS. This was quantified by two statistics: the abundance of galaxies as a function of stellar mass $\Phi(M_*)$, which we estimated over the stellar mass range $10^8 < M_* < 10^{12}h^{-2}M_\odot$, and the projected stellar mass autocorrelation function $w_p^*(r_p)$, which we estimated over the projected separation range $10h^{-1}\text{kpc} < r_p < 30h^{-1}\text{Mpc}$. Both statistics were robustly and precisely de-

* E-mail: leech@mpa-garching.mpg.de

terminated for the masses and scales probed. We found $w_p^*(r_p)$ to be remarkably well described by a power law, a behaviour which is approximately, but not perfectly reproduced by existing galaxy formation models. These measurements have been used in Guo et al. (2009) to link the stellar masses of galaxies to the dark matter masses of their haloes.

In this short paper we extend the work of Paper I by estimating projected *luminosity* autocorrelation functions. We use exactly the same methodology and the same galaxy sample as in Paper I. We compute luminosity autocorrelation functions for the five passbands of SDSS, and compare these with the stellar mass autocorrelation function obtained in Paper I. For each case we provide the parameters of the best-fitting power-law. By taking ratios of these autocorrelations we investigate the scale-dependence of the mean colours and mean mass-to-light ratios of clustered stellar populations. Finally, we discuss briefly how our results relate to other measures of the distribution of stellar light and mass in the low-redshift Universe.

2 STELLAR LUMINOSITY AUTOCORRELATION FUNCTIONS

We use the same galaxy sample as in Paper I except that we have dropped those galaxies with r -band absolute magnitude outside the range $-16 < M_{0.1,r} < -24$ or with poorly determined magnitudes in any of the other SDSS photometric bands. This reduces the sample by less than 1% (of which less than 0.2% is due to rejection of galaxies with poor photometry in bands other than r) so that it now consists of 482,755 galaxies. We use SDSS Petrosian magnitudes so that for each galaxy the luminosities, colours and stellar mass are all measured within a single well-defined aperture (defined to be twice the r -band Petrosian radius). Our methodology for estimating projected autocorrelation functions and for constructing the random sample necessary for such estimates is also identical to that in Paper I: the stellar masses of the pair members, $M_{*,i}$ and $M_{*,j}$ in Eqs. 3-5 of Paper I, are simply replaced by the corresponding luminosities, $L_{\alpha,i}$ and $L_{\alpha,j}$. Here α denotes the passband being considered which is one of the five bands of SDSS: u , g , r , i , or z . The luminosities are K -corrected to their values at $z = 0.1$ (see Blanton et al. 2003a; Blanton & Roweis 2007), and are corrected for evolution following Blanton et al. (2003b).

Our estimates of the projected luminosity autocorrelation functions, $w_p^L(r_p)$, are plotted in Fig. 1 for the five SDSS bands and are compared with the projected stellar mass function, $w_p^*(r_p)$. Error bars on $w_p^*(r_p)$ are estimated from the scatter between the results found when exactly the same methodology is applied to our 20 mock SDSS samples (see Paper I for details). We do not attempt to put independent error bars on the projected luminosity autocorrelations because with our technique the set of galaxy pairs used to estimate each of these functions is *exactly* the same, both in the real data and in the mock catalogues. As a result, the realisations of sampling noise, large-scale structure noise (“cosmic variance”) and background subtraction noise are identical in all our autocorrelation estimates. Only the colour and stellar mass-to-light ratio distributions of individual pair members are differently sampled for the different functions. Since very large numbers of galaxies contribute to each autocorrelation

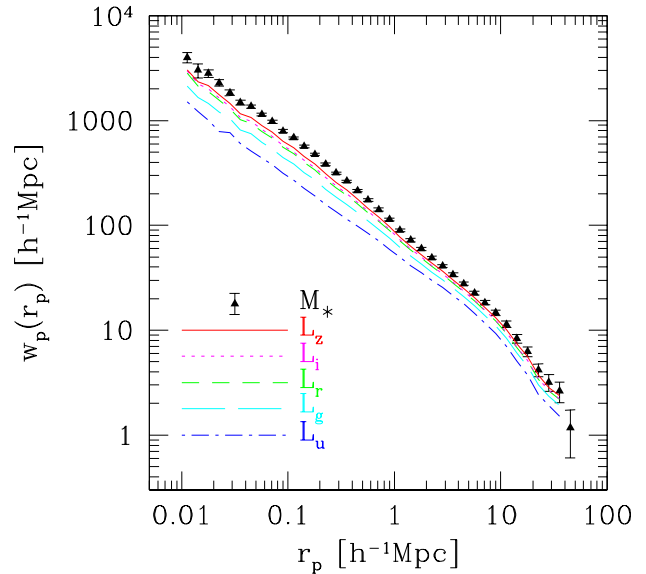


Figure 1. The projected stellar mass autocorrelation function in the SDSS is plotted as triangles with error bars and is compared to the projected luminosity autocorrelation functions measured for the five passbands of SDSS (the lines). Errors on the stellar mass autocorrelation function are estimated from the scatter among the measurements from 20 mock galaxy catalogues constructed from the Millennium Simulation (Springel et al. 2005) using the same selection criteria as the real sample.

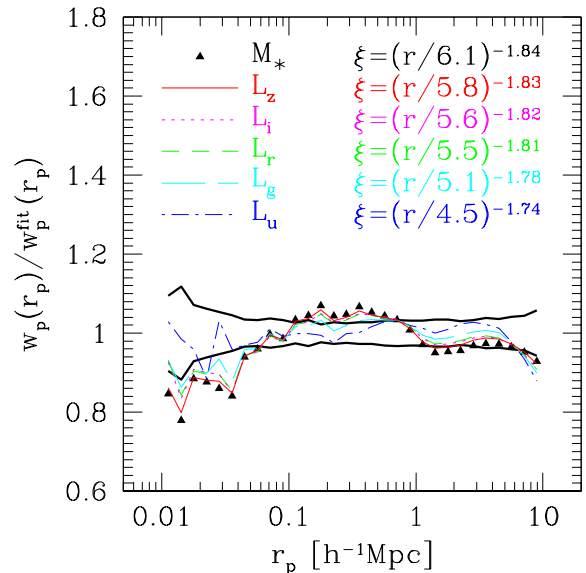


Figure 2. Ratio of the projected stellar mass (triangles) or luminosity (thin lines) autocorrelation functions in the SDSS to the individual best fit power-laws over the range $10 h^{-1} \text{kpc} < r_p < 10 h^{-1} \text{Mpc}$. The correlation length r_0 and the power-law slope γ of the corresponding three-dimensional autocorrelation function $\xi(r) = (r/r_0)^\gamma$ are indicated. The thick lines above and below unity indicate the $1-\sigma$ scatter of the stellar mass autocorrelation functions estimated from 20 mock galaxy catalogues constructed from the Millennium Simulation (Springel et al. 2005) to have the same selection effects as the real sample.

estimate and these distributions are narrow, they do not contribute significantly to the error budget.

Fig. 1 shows that luminosity clusters less strongly than stellar mass on all scales, regardless of which waveband we consider. Furthermore, the amplitude of clustering increases systematically with increasing wavelength on all scales.

Between $10h^{-1}\text{kpc}$ and $10h^{-1}\text{Mpc}$ the autocorrelation estimates are all well described by power laws. This is shown more clearly in Fig. 2 where we plot the ratio of each to the power law that best fits the set of estimates over this r_p range. Values of r_0 and γ for the corresponding three-dimensional autocorrelation functions $\xi(r) = (r/r_0)^\gamma$ are indicated in the figure. The result for the stellar mass correlation function is plotted as triangles for comparison. Note that these power laws should be considered as representations of our direct $w_p(r_p)$ estimates, rather than as a “best-fit” power law model for the underlying population correlations. Estimating the latter would require specification of a full clustering model up to at least fourth order, as well as careful consideration of the strong covariance between estimates of $w_p(r_p)$ on different scales. The two thick lines indicate the $1 - \sigma$ scatter about the mean for stellar mass correlation functions estimated from 20 mock SDSS samples constructed from the Millennium Simulation (Springel et al. 2005; Croton et al. 2006). The *rms* deviations from a power law are 4, 5, 6, 6, 7 and 7 percent for the *u*, *g*, *r*, *i* and *z* band autocorrelations and for the stellar mass autocorrelation, respectively. These are quite comparable to the *rms* uncertainty of 5 percent which we estimate for all these autocorrelations from our 20 mock catalogues over the same r_p range.

There is an apparent transition in the $w_p(r_p)$ estimates at about $1h^{-1}\text{Mpc}$. This is easily understood within the Halo Occupation Distribution (HOD) formalism as a consequence of the fact that pairs at larger separations almost all consist of galaxies which are members of two different halos (e.g. Cooray & Sheth 2002). On smaller scales the autocorrelation functions become steeper with increasing wavelength. This is the regime where there is a substantial contribution from pairs which are members of the same halo and the change in shape may reflect a colour-dependence of the weights given to halos of different mass, a colour-dependence of the distribution of galaxies within a given halo, or (more likely) both.

We have also estimated luminosity cross-correlations among the five bands. The cross-correlation between two bands is very nearly, but not exactly, equal to the geometric mean of the corresponding auto-correlations. The former is lower than, but within 2% of the latter for all r_p between $\sim 50 h^{-1}\text{kpc}$ and $\sim 20 h^{-1}\text{Mpc}$ and for all band pairs that do not involve the *u*-band. For cross-correlations involving *u*, the maximum difference is just below 3%. Thus, cross-correlations do not add much information beyond that contained in auto-correlations when characterizing the dependence of stellar populations on environment.

One may be concerned that systematic effects in the SDSS photometry might significantly bias our correlation results. We have carried out two tests to investigate possible systematics suggested by our referee. The SDSS Petrosian magnitudes are known to miss a larger fraction of total galaxy light in early- than in late-type galaxies. Since early-type galaxies are more strongly clustered, this might

lead us to underestimate small-scale clustering. For the first test we repeat our analysis replacing Petrosian magnitudes by the corresponding “model magnitudes” given for each galaxy in the SDSS catalogues. These are estimates of the total light, based on fits to the individual luminosity profiles. The resulting correlation measurements are all higher than, but within 3% of the Petrosian-based values for all r_p above $\sim 50 h^{-1}\text{kpc}$ and for all bands except *g*. For the *g*-band, the maximum difference in the luminosity autocorrelation is still less than 5%, and occurs for r_p between $\sim 100 h^{-1}\text{kpc}$ and $\sim 1 h^{-1}\text{Mpc}$. A second possible systematic concerns the well-known problem that the SDSS photometry tends to overestimate the sky background (and thus underestimate the luminosity) for large objects in crowded fields, in particular for brightest cluster galaxies. Again this could lead to systematic underestimates of small-scale correlations. We test the plausible size of this effect by increasing the luminosities of all galaxies more massive than $10^{11} M_\odot$ by 0.1 mag, the mean correction derived by von der Linden et al. (2007) for nearby brightest cluster galaxies (BCGs) larger than $20''$. The resulting correlation functions all remain within 2% of the “uncorrected” functions on all scales. Thus, at least these two systematics appear likely to affect our results by no more than a few percent.

3 COLOUR AND STELLAR MASS-TO-LIGHT RATIO DISTRIBUTIONS

If we take the ratio of our projected luminosity autocorrelation functions in two bands, for example *u* and *g*, we can write

$$\begin{aligned} w_p^{L_u}(r_p)/w_p^{L_g}(r_p) &= \frac{\langle L_{u,1}L_{u,2} \rangle_{r_p} / \langle L_u \rangle^2}{\langle L_{g,1}L_{g,2} \rangle_{r_p} / \langle L_g \rangle^2} \\ &= \frac{\langle (L_{u,1}/L_{g,1})(L_{u,2}/L_{g,2})L_{g,1}L_{g,2} \rangle_{r_p}}{\langle L_{g,1}L_{g,2} \rangle_{r_p}} \\ &\quad \div \frac{\langle (L_u/L_g)L_g \rangle^2}{\langle L_g \rangle^2}, \end{aligned}$$

where $\langle \dots \rangle_{r_p}$ denotes an average over all *correlated* pairs of galaxies with projected separation r_p , and $\langle \dots \rangle$ denotes an average over all individual galaxies. The second equality here shows that this autocorrelation ratio can be thought of as the luminosity-weighted (hence, approximately, per star weighted) average of the product of the luminosity ratios L_u/L_g of the pair members, relative to the square of the luminosity-weighted average of the same ratio for individual galaxies. Hence we can define a characteristic host galaxy colour for pairs of stars separated by r_p through, for example,

$$(u - g) - \langle u - g \rangle = -1.25 \log_{10}(w_p^{L_u}(r_p)/w_p^{L_g}(r_p)). \quad (1)$$

This quantity is shown in Fig. 3 as a function of r_p for the four colour indices defined by neighboring pairs of SDSS filters. The results are consistent with host galaxy colour being independent of scale both at large ($r_p >$ a few Mpc) and at small ($r_p <$ a few 100 kpc) separations. The scale-dependence at intermediate separations is strongest for $^{0.1}(u - g)$ although even here it amounts to a total variation of less than 0.1 magnitudes. The variation in colour is weaker for redder colours and is essentially absent for the reddest bands.

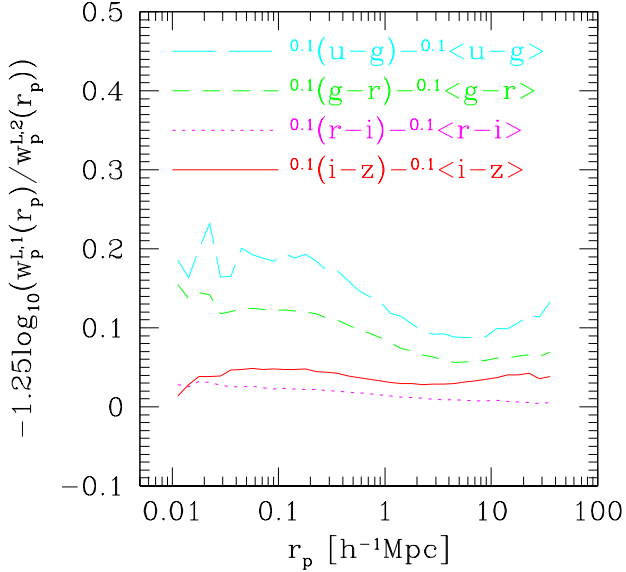


Figure 3. Mean colours of all correlated stars at projected distance r_p from a randomly chosen star relative to the luminosity-weighted average values of individual galaxies. These can be estimated directly from ratios of the projected autocorrelation functions in Fig. 1.

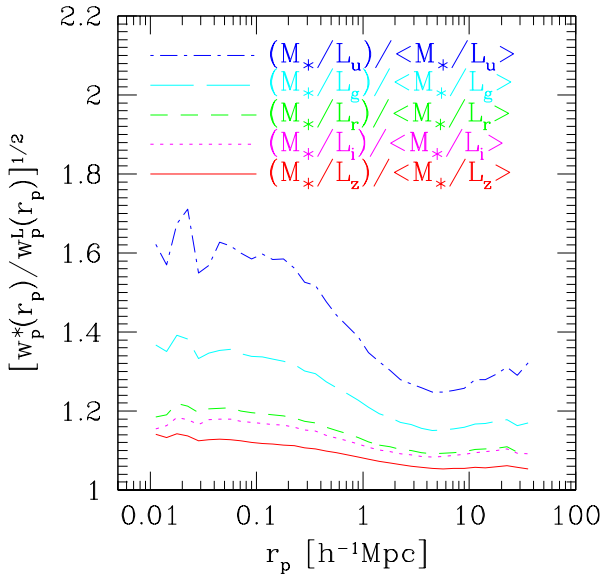


Figure 4. Mean mass-to-light ratios for all correlated stars at distance r_p from a randomly chosen star relative to the luminosity-weighted average values for individual galaxies. These can be estimated directly from ratios of the stellar mass and light autocorrelations in Fig. 1.

Replacing the luminosity autocorrelation function in the numerator of Eq. 1 by the projected stellar mass autocorrelation function produces an estimate of (the square of) the typical mass-to-light ratio of the host galaxies of (correlated) star pairs separated by r_p , relative to the luminosity-weighted average value for individual galaxies. We plot this

quantity for the five SDSS photometric bands in Fig. 4. The scale-dependence of M_*/L is similar to that of the colours: a transition to lower values occurs between a few 100 kpc and a few Mpc, but M_*/L is independent of scale on both smaller and larger scales. Again effects are strongest in u and get weaker with increasing wavelength, but in this case a small but significant trend is seen even in the z -band. M_*/L_u increases by about 25% from large to small scales.

The trends shown in this section are all easily understood as reflecting the fact that pairs of small separation are typically members of the same halo, whereas pairs at large separation must belong to different halos. This results in a different weighting with halo mass in the two regimes. In particular, close (‘one halo’) pairs are more strongly weighted towards massive halos than are distant (‘two halo’) pairs. In the former case at least one of the two galaxies must be a satellite object, whereas in the latter case both galaxies are often the central galaxy of their own halo. These trends result in a greater contribution from early-type “red-and-dead” galaxies to the small-scale correlations.

4 DISCUSSION

Just as was the case for the projected stellar mass autocorrelation function presented in Paper I, projected autocorrelation functions of luminosity in each of the five SDSS bands are robustly and precisely determined by our methods for $r_p < 30h^{-1}\text{Mpc}$. Over the full nonlinear range $10h^{-1}\text{kpc} < r_p < 10h^{-1}\text{Mpc}$, our estimates are all extremely well represented by power laws, corresponding to three-dimensional autocorrelation functions with parameters r_0 and γ which vary slightly but systematically from band to band. As pointed out in Paper I, this near power-law behaviour of the estimates must be seen as a coincidence because different physical and statistical processes control correlations in the small-scale (‘one-halo’) and large-scale (‘two-halo’) regimes. In our standard structure formation model there is no reason why these should conspire to produce a single power law. If the “one-galaxy” term in the mass and luminosity autocorrelations were included, there would be a strong upward break at $r_p \sim 10h^{-1}\text{kpc}$, the scale of individual galaxies.

Our luminosity autocorrelation estimates quantify the extent to which the spatial distribution of optical light in the local Universe depends on scale and wavelength. The relative bias between the longest and shortest wavebands varies from a factor of 1.5 on small scales ($< 100\text{kpc}$) to a factor of 1.2 on large scales ($> \text{a few Mpc}$). Luminosity in all bands and on all scales clusters less strongly than stellar mass, although for z -band luminosity the difference is small. This is expected because z -band light is known to be closely related to stellar mass indicators (e.g. Kauffmann et al. 2003).

All the autocorrelation functions considered in this paper have very similar shape on large scales ($> 5\text{Mpc}$). This is expected in models where the properties of galaxies depend on the detailed formation history within their own dark matter halos, but are independent of the formation histories of distant halos. On smaller scales the shape of the various autocorrelation functions differ, reflecting differences in the relative strength of the one-halo and two-halo contributions which arise from a combination of effects. One-halo

correlations are more heavily weighted towards massive halos than are two-halo correlations, and red and high M_*/L galaxies are typically found in more massive halos than blue galaxies of similar mass. Small-scale correlations are also sensitive to how satellite galaxies are distributed with radius within their dark halos (see Weinmann et al. 2006 and von der Linden et al. 2009 for recent observational studies demonstrating that these radial distributions do indeed depend on galaxy colour and M_*/L). The precise quantitative results we obtain in this paper, when combined with accurate luminosity and stellar mass functions, provide a compact way to constrain Halo Occupation Distribution models which try to represent all these relations in detail (e.g. Watson et al. 2009).

The mass/luminosity auto-correlation functions considered here are quite closely related to the marked correlation functions considered by others (MCF; e.g. Beisbart & Kerscher 2000; Faltenbacher et al. 2002; Sheth 2005; Skibba et al. 2006; Skibba & Sheth 2009; Skibba et al. 2009). The two statistics weight data-data (DD) pairs in a similar way, but are usually estimated and presented differently. In the case of the MCF, one doesn't normally measure the weighted correlation function (WCF) in the way we do, but rather estimates the ratio $(1+WCF)/(1+UCF)$ simply by comparing the weighted DD count with the unweighted one (UCF here represents the unweighted correlation function). The advantage is that one doesn't need to construct random samples in order to count random-random (RR) and data-random (DR) pairs. A disadvantage for projected correlations of the kind we have studied, is that the resulting estimate depends explicitly not only on the 3-dimensional clustering process, but also on sample selection procedures and the way the redshift separation of pairs is limited. Recently, Skibba et al. (2009) have partially addressed this last issue by estimating weighted and unweighted projected CFs, $W_p(r_p, \pi)$ and $w_p(r_p, \pi)$, integrating them over a fixed range in π , and then constructing the equivalent of a standard MCF as the ratio $[1 + W_p(r_p)/r_p]/[1 + w_p(r_p)/r_p]$. As with more traditional estimates, this 'MCF' goes to unity on large (linear) scales and so tends to obscure interesting information there about the relative bias of light, mass or other 'marks', e.g. the variation in colour and M_*/L among bands shown in Figs. 3 and 4.

ACKNOWLEDGMENTS

The authors thank an anonymous referee for helpful comments. CL is supported by the Joint Postdoctoral Programme in Astrophysical Cosmology of Max Planck Institute for Astrophysics and Shanghai Astronomical Observatory, by NSFC (10533030, 10633020), by 973 Program (No.2007CB815402) and by the Knowledge Innovation Program of CAS (No.KJXC2-YW-T05).

Funding for the SDSS and SDSS-II has been provided by the Alfred P. Sloan Foundation, the Participating Institutions, the National Science Foundation, the U.S. Department of Energy, the National Aeronautics and Space Administration, the Japanese Monbukagakusho, the Max Planck Society, and the Higher Education Funding Council for England. The SDSS Web Site is <http://www.sdss.org/>.

The SDSS is managed by the Astrophysical Research

Consortium for the Participating Institutions. The Participating Institutions are the American Museum of Natural History, Astrophysical Institute Potsdam, University of Basel, University of Cambridge, Case Western Reserve University, University of Chicago, Drexel University, Fermilab, the Institute for Advanced Study, the Japan Participation Group, Johns Hopkins University, the Joint Institute for Nuclear Astrophysics, the Kavli Institute for Particle Astrophysics and Cosmology, the Korean Scientist Group, the Chinese Academy of Sciences (LAMOST), Los Alamos National Laboratory, the Max-Planck-Institute for Astronomy (MPIA), the Max-Planck-Institute for Astrophysics (MPA), New Mexico State University, Ohio State University, University of Pittsburgh, University of Portsmouth, Princeton University, the United States Naval Observatory, and the University of Washington.

REFERENCES

- Abazajian K. N., Adelman-McCarthy J. K., Agüeros M. A., Allam S. S., Allende Prieto C., An D., Anderson K. S. J., Anderson S. F., et al., 2009, *ApJS*, 182, 543
 Beisbart C., Kerscher M., 2000, *ApJ*, 545, 6
 Benoist C., Maurogordato S., da Costa L. N., Cappi A., Schaeffer R., 1996, *ApJ*, 472, 452
 Blanton M. R., Brinkmann J., Csabai I., Doi M., Eisenstein D., Fukugita M., Gunn J. E., Hogg D. W., et al., 2003a, *AJ*, 125, 2348
 Blanton M. R., Hogg D. W., Bahcall N. A., Brinkmann J., Britton M., Connolly A. J., Csabai I., Fukugita M., et al., 2003b, *ApJ*, 592, 819
 Blanton M. R., Lupton R. H., Schlegel D. J., Strauss M. A., Brinkmann J., Fukugita M., Loveday J., 2005, *ApJ*, 631, 208
 Blanton M. R., Roweis S., 2007, *AJ*, 133, 734
 Boerner G., Mo H., Zhou Y., 1989, *A&A*, 221, 191
 Brown M. J. I., Webster R. L., Boyle B. J., 2000, *MNRAS*, 317, 782
 Cooray A., Sheth R., 2002, *Phys.Rep.*, 372, 1
 Croton D. J., Springel V., White S. D. M., De Lucia G., Frenk C. S., Gao L., Jenkins A., Kauffmann G., et al., 2006, *MNRAS*, 365, 11
 Davis M., Geller M. J., 1976, *ApJ*, 208, 13
 Davis M., Meiksin A., Strauss M. A., da Costa L. N., Yahil A., 1988, *ApJ*, 333, L9
 Dressler A., 1980, *ApJ*, 236, 351
 Einasto M., 1991, *MNRAS*, 252, 261
 Faltenbacher A., Gottlöber S., Kerscher M., Müller V., 2002, *A&A*, 395, 1
 Guo Q., White S., Li C., Boylan-Kolchin M., 2009, *ArXiv e-prints*
 Guzzo L., Strauss M. A., Fisher K. B., Giovanelli R., Haynes M. P., 1997, *ApJ*, 489, 37
 Hamilton A. J. S., 1988, *ApJ*, 331, L59
 Kauffmann G., Heckman T. M., White S. D. M., Charlot S., Tremonti C., Brinchmann J., Bruzual G., Peng E. W., et al., 2003, *MNRAS*, 341, 33
 Kauffmann G., White S. D. M., Heckman T. M., Ménard B., Brinchmann J., Charlot S., Tremonti C., Brinkmann J., 2004, *MNRAS*, 353, 713

- Li C., Jing Y. P., Kauffmann G., Börner G., White S. D. M., Cheng F. Z., 2006, *MNRAS*, 368, 37
- Li C., White S. D. M., 2009, *MNRAS*, 398, 2177
- Loveday J., Maddox S. J., Efstathiou G., Peterson B. A., 1995, *ApJ*, 442, 457
- Norberg P., Baugh C. M., Hawkins E., Maddox S., Peacock J. A., Cole S., Frenk C. S., Bland-Hawthorn J., et al., 2001, *MNRAS*, 328, 64
- Park C., Vogeley M. S., Geller M. J., Huchra J. P., 1994, *ApJ*, 431, 569
- Sheth R. K., 2005, *MNRAS*, 364, 796
- Skibba R., Sheth R. K., Connolly A. J., Scranton R., 2006, *MNRAS*, 369, 68
- Skibba R. A., Bamford S. P., Nichol R. C., Lintott C. J., Andreescu D., Edmondson E. M., Murray P., Raddick M. J., et al., 2009, *MNRAS*, 399, 966
- Skibba R. A., Sheth R. K., 2009, *MNRAS*, 392, 1080
- Springel V., White S. D. M., Jenkins A., Frenk C. S., Yoshida N., Gao L., Navarro J., Thacker R., et al., 2005, *Nature*, 435, 629
- Swanson M. E. C., Tegmark M., Blanton M., Zehavi I., 2008, *MNRAS*, 385, 1635
- von der Linden A., Best P. N., Kauffmann G., White S. D. M., 2007, *MNRAS*, 379, 867
- von der Linden A., Wild V., Kauffmann G., White S. D. M., Weinmann S., 2009, *ArXiv e-prints*
- Wang Y., Yang X., Mo H. J., van den Bosch F. C., 2007, *ApJ*, 664, 608
- Watson D. F., Berlind A. A., McBride C. K., Masjedi M., 2009, *ArXiv e-prints*
- Weinmann S. M., van den Bosch F. C., Yang X., Mo H. J., 2006, *MNRAS*, 366, 2
- White S. D. M., Tully R. B., Davis M., 1988, *ApJ*, 333, L45
- Willmer C. N. A., da Costa L. N., Pellegrini P. S., 1998, *AJ*, 115, 869
- York D. G., Adelman J., Anderson Jr. J. E., Anderson S. F., Annis J., Bahcall N. A., Bakken J. A., Barkhouser R., et al., 2000, *AJ*, 120, 1579
- Zehavi I., Blanton M. R., Frieman J. A., Weinberg D. H., Mo H. J., Strauss M. A., Anderson S. F., Annis J., et al., 2002, *ApJ*, 571, 172
- Zehavi I., Zheng Z., Weinberg D. H., Frieman J. A., Berlind A. A., Blanton M. R., Scoccamarro R., Sheth R. K., et al., 2005, *ApJ*, 630, 1

This paper has been typeset from a \TeX / \LaTeX file prepared by the author.